

Precision Stationkeeping with Azimuthing Thrusters

by

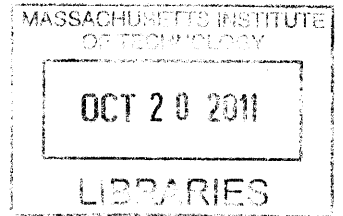
Adam D. Doroski

SUBMITTED TO THE DEPARTMENT OF MECHANICAL ENGINEERING IN
PARTIAL FULFILLMENT OF THE REQUIREMENTS FOR THE DEGREE OF

BACHELOR OF SCIENCE IN MECHANICAL ENGINEERING
AT THE
MASSACHUSETTS INSTITUTE OF TECHNOLOGY

JUNE 2011

The author hereby grants to MIT permission to reproduce and to
distribute publicly paper and electronic copies of this thesis
document in whole or in part in any medium now known or
hereafter created.



ARCHIVES

© Massachusetts Institute of Technology 2011. All rights reserved.

Signature of Author: _____

Department of Engineering
May 17, 2011

Certified by: _____

Franz Hover
Finmeccanica Career Development Professor of Engineering
Thesis Supervisor

Accepted by: _____

John H. Lienhard V
Collins Professor of Mechanical Engineering
Chairman, Undergraduate Thesis Committee

[This page intentionally left blank.]

Precision Stationkeeping with Azimuthing Thrusters

by

Adam D. Doroski

Submitted to the Department of Mechanical Engineering
on May 17, 2011 in partial fulfillment of the
requirements for the Degree of Bachelor of Science in
Mechanical Engineering

ABSTRACT

Precision positioning of an unmanned surface vehicle (USV) in a nautical environment is a difficult task. With a dual azimuthing thruster scheme, the optimization of thruster outputs uses an online method to minimize the amount of error. It simplifies necessary calculations by the assumption that the rotating thrusters are always parallel thus making the system holonomic. The scheme accommodates for limitations in actuator outputs, including rotation limits and time-lagged thrusts and was implemented in a MATLAB simulation that tested its response to step errors and disturbance forces, similar to what it would encounter in actual implementation. It successfully achieved commanded outputs in all three degrees of freedom, typically within 25 seconds. It also rejects constant and sinusoidal disturbance forces. However, specific configurations arise where the USV, at times, is uncontrollable and the system only recovers after being further perturbed into a controllable configuration.

Thesis Supervisor: Franz Hover
Title: Professor of Mechanical Engineering

Table of Contents

		Page No.
i.	Cover Page	1
ii.	Abstract	3
iii.	Table of Contents	4
1.	Introduction	5
	1. Autonomous Underwater Sensing Networks	5
	2. Unmanned Surface Vehicle Station Keeping	6
2.	Background	7
	1. Azimuthing Thrusters	7
	2. Coordinate System Overview	8
	3. Stationkeeping and Kayak Orientation	10
	4. Open Loop System Dynamics	11
	5. Feedback Control and the PID Controller	14
3.	Methods	16
	1. MATLAB Model and Simulation	16
	2. Quantifying Controller Performance	17
	3. Experimental Controller	18
4.	Simulation Process and Results	18
	1. Digression on Data Presentation	19
	2. One and Two Degree of Freedom Step Responses	20
	3. Oscillatory and Damped Three Degree of Freedom Responses	21
	4. Response to Constant Disturbance Force	22
	5. Response to Sinusoidal Disturbance Force	23
	6. Operation near Azimuthing Thruster Physical Stop	25
5.	Analysis and Discussion	26
	1. Predictive Nature of the Azimuthing Thrusters	26
	2. Transient Error Reduction	28
	3. Failure Conditions of the Controller	29
	4. Thruster Response	30
6.	Conclusion	31
7.	Acknowledgements	32
8.	Appendices	
	A. Formation of State Space Matrices	33
	B. Derivation of Controller Outputs	35
	C. Example PD Constant Iteration	37
	D. Application and Formation of Disturbance Forces	39

1. Introduction

In recent years, distributed sensor networks (DSNs) have become an important area of research for military and commercial applications. Distributed sensing utilizes groups of smaller sensors to monitor an environment as opposed to one larger sensor¹. These smaller sensors can be placed on mobile platforms that allow the network to move and adapt to a specific environment as necessary. The coordination of these platforms and the consolidation of sensor data is an essential implied task within sensor networks.

Specific environments prove to be more of a challenge to distributed sensing than others. Efforts to characterize underwater environments require the use of autonomous underwater vehicles (AUVs), which are limited in many ways compared to above ground platforms. In order to link an underwater network to a surface network (so that data can be utilized in a research or commercial application), a mobile gateway craft is used. This craft needs to move and position itself precisely relative to the underwater network. Unmanned surface vehicles (USVs) are able to maneuver with underwater sensing networks and relay data between the swarm and users. Precision positioning, known as stationkeeping, enables the craft to optimally coordinate with the underwater network.

1.1 Autonomous Underwater Sensing Networks

Operating in an underwater environment places many constraints on DSNs. Aside from the obvious (but not trivial) need to be water-tight and battery powered, AUVs suffer from having to communicate on the acoustic channel². DSNs, especially mobile ones, require an efficient and capable channel of communication to transmit not only sensor data, but also data regarding the specific AUV's characteristics, whether it is physical location or battery life remaining. The AUV must also be able to receive commands in order to effectively collect environment data. Underwater acoustic communication has much lower bandwidth and higher packet loss compared to wireless communication above ground. It also operates over much shorter ranges, further requiring that any gateway craft position themselves optimally to consolidate data.

¹ Iyengar, S. S., Seetharaman, G., Kannan, R., Durresi, A., Park, S., Khrisnamanchari, B., et al. (2004). Next generation distributed sensor networks. *Proceedings of the Office of Naval Research*, September 5–6. USA

² Jim Partan, Jim Kurose, and Brian Neil Levine. 2007. A survey of practical issues in underwater networks. *SIGMOBILE Mob. Comput. Commun. Rev.* 11, 4 (October 2007), 23-33.

1.2 Unmanned Surface Vehicle Station Keeping

A mobile surface vehicle is capable of serving as both a gateway and a physical reference point for an AUV or a group of AUVs and move with them. The USV's ability to stationkeep is an important, basic capability needed by any such AUV-following surface vehicle.

In maneuvering the craft, a stationkeeping controller needs to weigh the importance of transient error in achieving its final position versus the settling time to that position. For traditional, under-actuated, surface vehicle thruster layouts (such as with propeller and rudder), it is almost impossible to achieve a given position without first maneuvering the boat away from the target³. Other arrangements, such as the inclusion of transverse thrusters, increase the range of directions that the craft can move. However, additional thrusters may lead to over-actuation where the number of actuators is greater than the number of degrees of freedom.

A basic scheme of the problem is shown in block diagram form below. Ideally, the craft's current position is compared to the desired position (ideally refers to the fact that it is difficult to exactly measure the craft's position). The online controller computes the appropriate actuator commands which are fed into a motor controller interface and then acted on by the craft.

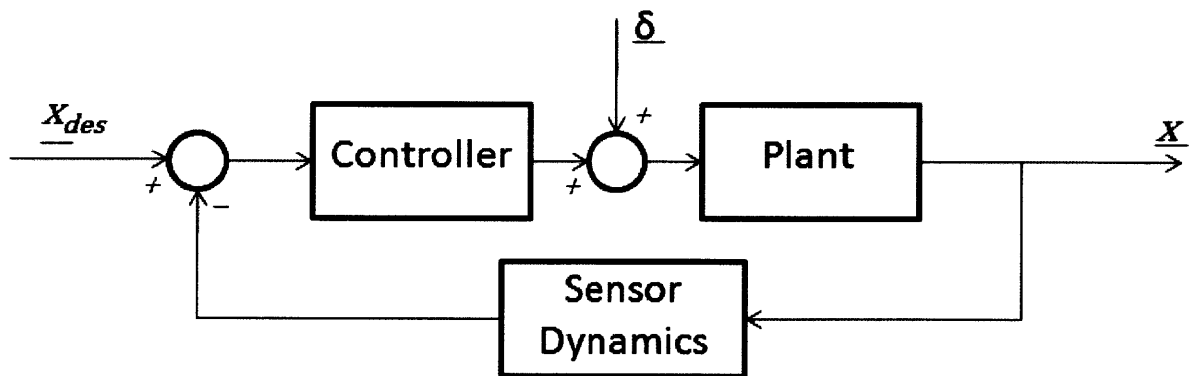


Figure 1.1: Block diagram describing the feedback control loop and disturbance forces.

³ Pereira, A.; Das, J.; Sukhatme, G.S.; , "An experimental study of station keeping on an underactuated ASV," *Intelligent Robots and Systems, 2008. IROS 2008. IEEE/RSJ International Conference on* , vol., no., pp.3164-3171, 22-26 Sept. 2008

In addition to the controller outputs being fed into the kayak system, disturbance forces $\underline{\delta}$ also affect the behavior of the kayak. This can be in the form of surface disturbances, such as wind and wave interactions, or underwater currents.

In simple forms of stationkeeping such as the case where one only corrects craft heading and disregards location, the control problem is simplified. The rudder and propeller example, an under-actuated situation, is now fully actuated because the boat is able to change heading without care of translational errors.

2. Background

The structure of the gateway craft capable of bridging between an underwater sensing network and the surface environment is a light-weight, recreation kayak with fore and aft azimuthing thrusters. It is a Wave Sport© Fuse 35 model personal kayak, custom modified to house the thrusters, controller, sensors, and batteries necessary.



Figure 2.1: Profile of HoverGroup kayak with bow and aft azimuthing thrusters.

2.1 Azimuthing Thrusters

Azimuthing thrusters are thrusters that are capable of rotating relative to the craft in order to produce surge and/or sway forces. Compared to other control surfaces, such as propellers, tunnel thrusters, and rudders, azimuthing thrusters offer the most amount of variability because of their ability to rotate given different vehicle states⁴. The extra degree of freedom often leads

⁴ T.I. Fossen, T.A. Johansen, "A Survey of Control Allocation Methods for Ships and Underwater Vehicles," Mediterranean Conference on Control and Automation, pp. 1-6, 2006 14th Mediterranean Conference on Control and Automation, 2006

to over-actuated schemes that are solved with different minimization schemes, traditionally through power conservation.

Although sophisticated azimuthing thrusters exist, many basic units are limited in the angle they can traverse. This non-linearity is typically accommodated for in control laws by “penalizing” the thruster from reaching the end of its range. This penalty is assessed when minimizing an appropriate cost function of actuator behavior. Azimuthing thrusters are further limited by the rate at which they are able to rotate, which is adjusted for in a similar fashion.

The azimuthing thrusters utilized by this kayak are custom engineered to fit into the craft. The “thrusters” can be divided into two motors: the thruster which propels the kayak and the servo which rotates the thruster. Throughout this study, it is assumed that the thrusters can only create positive thrust. Furthermore, the dynamics of the thruster induce a time-lagged effect on the force output.

The servo uses a custom-engineered housing that couples the thruster spindle to the servo. Due to the design of the thruster, it does not utilize this full range for fear of damaging the electrical connections that run through the thruster shaft. However, there is no feedback from the servo indicating that it has reached the correct position, making it unobservable.

2.2 Coordinate System Overview

Nautical vehicles have six degrees of freedom, corresponding to movement in three translational planes and three rotational frames. From a body-referenced frame, the three translations are surge, sway, and heave and are related to the heading of the vehicle as shown in Figure 2.2.

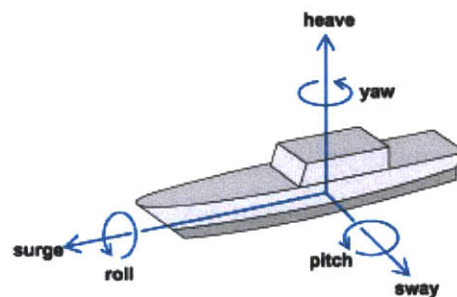


Figure 2.2: Depiction of nautical craft degrees of freedom. Image courtesy of Answers.com

Rotations about each of the three translational axis are also seen in Figure 2.2 and are known as roll, pitch, and yaw.

Since stationkeeping is a craft's ability to maintain a fixed location on the water's surface, it is useful to think of in a planar system, disregarding heave motions. Additionally, the heading of the vessel is controlled because the orientation of the craft is closely linked to the behavior of the system.

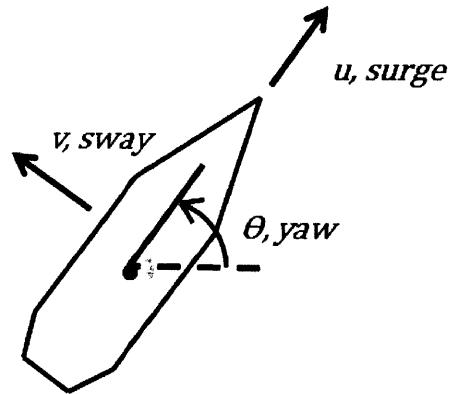


Figure 2.3: Body-referenced translational and rotational movement definitions of sway, surge, and yaw.

Surge, sway, and yaw are denoted by u , v , and θ , respectively. In order to track the position of the kayak as the body-frame moves, surge and sway are translated into Cartesian coordinates and integrated with respect to time.

Cartesian coordinates allow for easy computation of the position error while stationkeeping. In defining a nautical craft's range of attainable motions, it is more convenient to work in a body-referenced frame where vehicle translations are defined from its heading in that instant, known as surge and sway translations. It is traditionally easier for these vehicles to produce motions in line with their heading (surge) versus motions perpendicular to their heading (sway).

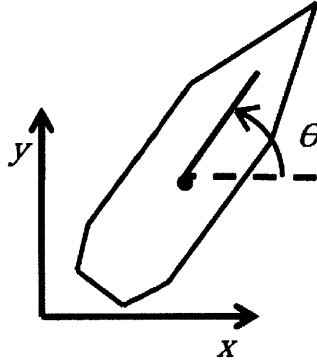


Figure 2.4: Absolute (fixed) Cartesian coordinate system used to analyze the system performance for position and error computations.

The azimuths, or angles, of the two thrusters are defined relative to the craft. These angles will be defined by α_1 , referring to the bow thruster, and α_2 , the aft thruster.

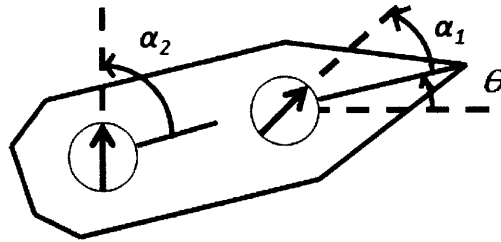


Figure 2.5: The angles of the azimuthing thrusters are defined relative to the heading of the craft.

Within the laboratory setting, the USV will be defined in a Cartesian system. It is important to note that θ is defined from the positive x -axis which would need to be accommodated for if a compass is used.

2.3 Stationkeeping and Kayak Orientation

With traditional vessels, it is much easier to move in line with the ship's heading compared to perpendicular to it. In order to move towards a destination, the vessel needs to align

the ship directly towards the target. This result is from two different effects: the common under-actuation of a vessel and the geometry of the ship⁵.

A kayak on the other hand is a highly-maneuverable craft. Although it does not move as easily perpendicular to its heading relative to inline with its heading, it can achieve movement in the sway direction with little trouble. Furthermore, a dual-azimuthing thruster layout, by definition, over-actuates the system and allows it to produce a wide range of forces and torques through the use of its thrusters angles and outputs.

However, certain thruster configurations should be avoided when the rotation limitations of the thrusters are analyzed. Consider the case where the kayak's thrusters are operating close to their position limit; in order to correct small perturbations in translational position, it may be necessary to move a full rotation in order to reach a configuration that was only a few degrees away. This leads to a period of time where the kayak is not fully controllable, capable of producing undesirable results.

Since the craft's range of motions is fairly large, the determination of where the limits of the thrusters are placed is not trivial. That is, if the kayak were not able to move in the sway direction, it would be obvious the place the limits perpendicular to the vessel. However, in the case of controlling three degrees of freedom, operating around the constraint is tough. If the constraint on one degree of freedom was momentarily relaxed (or "put off" to the future), the kayak can orient itself in such a way that it can avoid reaching the rotation limits of each thruster.

2.4 Open Loop System Dynamics

A set of three equations corresponding to the degrees of freedom of the kayak are used to characterize the system. After ignoring heave, pitch, and roll motions, the linear momentum equations in the surge u and sway v directions simplify to:

$$m\dot{u} - v\dot{\theta} = b_{surge}u + F_1 \cos \alpha_1 + F_2 \cos \alpha_2 + \delta_{surge} \quad (1)$$

$$m\dot{v} + u\dot{\theta} = b_{sway}v + F_1 \sin \alpha_1 + F_2 \sin \alpha_2 + \delta_{sway} \quad (2)$$

⁵ Hover, Franz, and Harrison Chin. *2.017J Design of Electromechanical Robotic Systems, Fall 2009*. (Massachusetts Institute of Technology: MIT OpenCourseWare), <http://ocw.mit.edu> (Accessed 09 May, 2011). License: Creative Commons BY-NC-SA

Here, the body-referenced frame is defined from the center of mass of the kayak. The angles of the thrusters, relative to the heading of the kayak, are denoted by α_1 and α_2 . These determine the amount of force, F_1 and F_2 , that is applied in each direction.

The angular momentum in the yaw direction also simplifies to:

$$I_{\theta\theta}\ddot{\theta} = b_{yaw}\dot{\theta} + F_1 l_1 \sin \alpha_1 - F_2 l_2 \sin \alpha_2 + \delta_{yaw} \quad (3)$$

where $I_{\theta\theta}$ is the craft's moment of inertia, l_1 and l_2 are vector lengths from the center of mass of the kayak to each thruster.

Viscous forces are handled by the assumption that there is three separate damping terms in the system; b_{surge} and b_{sway} refers to constant damping terms that slow translational motions and rotational velocity is restricted by b_{yaw} .

Disturbance forces can be found in all three equations. They are consolidated into a disturbance matrix $\underline{\delta}$ of the form:

$$\underline{\delta} = [\delta_{surge} \quad \delta_{sway} \quad \delta_{yaw}]^T \quad (4)$$

Tracking of the kayak's position is handled in the Cartesian frame. Surge and sway motions are related to x and y by the following relationship:

$$\begin{bmatrix} x \\ y \end{bmatrix} = \begin{bmatrix} x_0 \\ y_0 \end{bmatrix} + \int_0^t \underline{R} \begin{bmatrix} u \\ v \end{bmatrix} d\tau \quad (5)$$

where \underline{R} is a rotation matrix defined as:

$$\underline{R} = \begin{bmatrix} \cos \theta & -\sin \theta \\ \sin \theta & \cos \theta \end{bmatrix} \quad (6)$$

The rotational dynamics of the azimuthing thrusters are assumed to be of first order with limits on position and maximum angular velocity. Since the angles are not observable by the

controller, its position is controlled by designating a position slew rate that is smaller than the maximum angular velocity of the servo. The slew rate places a ceiling on speed at which it can rotate, not allowing it to exceed a given ω_i . For a thruster i ,

$$|\dot{\alpha}_i| = \min \left(\left| \frac{\alpha_{error,i}}{dt} \right|, \omega_i \right) \quad (7)$$

This can be interpreted as forcing the servo to move at its maximum speed ω_i if it cannot reach the desired location by the next time step. If it can reach the desired position, it moves at a speed exactly equal to the speed needed to achieve that location.

Inertial terms are ignored because the system is driven by a high-torque servo where the combined moments of inertia for the servo and the thruster are relatively small. Additionally, the servo contains an internal controller that works in series with the kayak controller; however, in actual implementation, the above assumption is adequate for the system.

The propeller dynamics also restrict the force a thruster can produce at a moment in time. It cannot instantly respond to changes in controller commands due to inertial and hydrodynamic forces. The propellers are assumed to produce a time-lagged thrust where the force for a thruster i at a moment in time t is:

$$F_{i,t} = \tau F_{i,t-1} + (1 - \tau) \tilde{F}_{i,t} \quad (8)$$

$$\tau \in [0,1] \quad (9)$$

where $\tilde{F}_{i,t}$ is the controller command at the current time, $F_{i,t-1}$ is the thruster force from the previous time step, and τ is a lag coefficient that determines how dramatic the change in force can be. If $\tau = 1$, the system is fully lagged and will never produce thrust, despite commands otherwise. Likewise, $\tau = 0$ leads to instant achievement of the commanded force.

The state vector that fully defines the system is an eighth order vector from the three vehicle degrees of freedom and the orientations of the two thrusters.

$$\underline{x} = [u \ v \ \dot{\theta} \ \alpha_1 \ \alpha_2 \ x \ y \ \theta]^T \quad (10)$$

In a state space framework, the derivative of the state vector $\underline{\dot{x}}$ can be described by the equation:

$$\underline{\dot{x}} = \underline{A} \underline{x} + \underline{F}(\underline{x}, \underline{u}) + \underline{\delta} \quad (11)$$

$$\underline{u} = [\alpha_1 \quad \alpha_2 \quad F_1 \quad F_2 \quad \alpha_{des,1} \quad \alpha_{des,2}]^T \quad (12)$$

which relates the system to its actuator outputs. \underline{A} and \underline{F} are derived from equations (1), (2) and (3) by solving for the second derivatives and is further explained in Appendix A. In addition, the \underline{F} matrix contains nonlinearities produced from the behavior of the thrusters as well as the effects that arise from changing the body-referenced frame to the absolute frame. It is not possible to analyze the system with linear algebra techniques but this notation does ease the description of the system.

2.6 Feedback Control and the PID Controller

Closing the loop of a system requires the observation of the system states. In order for a craft to reach or maintain a certain absolute position, a controller compares the destination matrix to its current state and feeds appropriate inputs back into the system. The system error is defined as:

$$\underline{E} = \begin{bmatrix} x_{des} - x \\ y_{des} - y \\ \theta_{des} - \theta \end{bmatrix} \quad (13)$$

where x_{des} , y_{des} , and θ_{des} , are user defined positions. \underline{E} is differentiable matrix with respect to time so that finer tuning of the system is possible. This implicitly requires that the derivatives of both the destination matrix and current state are observable.

In order to constantly drive the system to the destination matrix, the actuator outputs are defined so that they are proportional to the error matrix \underline{E} . With a PID controller, the response of the system can be controlled by modifying the three specific constants. The proportional and

derivative constants are used to shape the response of the system by scaling the error vector. The PID operator is defined by:

$$\underline{k} = \left[k_p \quad k_d \left(\frac{d}{dt} \right) \quad k_i \int_0^t d\tau \right] \quad (14)$$

and the scaled vector is:

$$\underline{T}(i) = \underline{k} \underline{E}(i) \quad (15)$$

where i corresponds to the three degrees of freedom x , y , and θ .

For the standard second order mass-spring-damper system, the three constants have specific roles in modifying the system. Two of these, proportional and damping, are more commonly used for characterizing the transient behavior of the system. The proportional constant k_p serves as a virtual spring constant to the system, adding or subtracting stiffness into the system. The derivative constant k_d acts as virtual damping, slowing the movement of the system and decaying oscillations.

The final term, k_i , serves mainly to correct steady state errors within the system. Steady state errors are often observed in controllers where a disturbance force acts on a system and is only balanced by proportional control instead of correcting it. By recording the error history, the integral term eventually decays the error to zero.

By analyzing the \underline{T} vector, a controller can specify the actuator outputs. The force outputs \underline{F} are related to the scaled error matrix by the configuration matrix \underline{C} :

$$\underline{T} = \underline{C} \underline{F} \quad (16)$$

where:

$$\underline{C} = \begin{bmatrix} \cos \alpha_1 & \cos \alpha_2 \\ \sin \alpha_1 & \sin \alpha_2 \\ l_1 \sin \alpha_1 & -l_2 \sin \alpha_2 \end{bmatrix} \quad (17)$$

Trying to solve equation (16) leads to three error and configuration equations with four actuator unknowns. A controller is able to solve for actuator outputs with additional, user defined constraints or through the use of a linear-quadratic regulator (LQR), which minimizes an appropriate cost function to solve for the fourth condition.

3. Methods

Analyzing the performance of a stationkeeping controller must be done from multiple perspectives. A controller must be able to maneuver into position and perform course corrections to remain in position. These can be simulated by two different situations: the case of a step input in one or more degree of freedoms and the case of a disturbance force vector perturbing the kayak away from its destination.

3.1 MATLAB Model and Simulation

In order to test the various controllers and situations, a forward Euler method model was created utilizing the dynamic equations discussed in Section 2.4. The time step can be varied to ensure that the calculated resulting solution is accurate as well as to reduce computational loads. Controlling the time step is also important in being able to simulate the limited update rate of the position sensors and limited output rate of the controller itself. This study found that a .1 second time step converged to smaller solutions calculated by .001 seconds. However, it was implemented with a .01 second time step.

The simulation calls upon the controller to be tested with the current system state \underline{x} , the desired position \underline{x}_{des} , and a vector of PID controller constants. The controller returns a specific set of actuator outputs that the model attempts to execute; it is possible that a “poor” controller specifies impossible outputs. The limitations imposed by the model include positive thrust only, a slew rate control over the thruster angular velocity, and only allowing one full rotation to operate over. Through iterating over various controller constants and the analysis of the kayak trajectory, the best performing controller can be implemented.

The model also allows for the simulation of disturbance forces that would lead to a steady state error in the kayak system. The disturbance force is simplified to a planar vector that varies in both the magnitude and direction according to a normal distribution. This randomness

perturbs the system in a more realistic way, hopefully exposing possible failure configurations in the actual implementation of the kayak.

3.2 Quantifying Controller Performance

In the design of a system, there are many common characteristics used to judge the behavior of the response. These include rise time, settling time, and percent overshoot, to name a few. In order to determine the efficiency of a system with more than one output, it would seem appropriate to sum or average these qualities and choose the best response.

For the kayak system, it is not obvious which characteristic is best; is it better to quickly settle to the location with oscillation or better to slowly decay towards the result? A more appropriate qualification of the system is weighted cumulative error (WCE). This accounts for error within the transient response as well as in the final response. Choosing the controller constants such that the weighted cumulative error is minimized also selects the controller with the best transient and steady-state responses.

The discrete-time formulation of the WCE is defined as:

$$WCE = \sum_{i=1}^n w_i (|x_{error}| + |y_{error}| + c|\theta_{error}|) \quad (18)$$

where n is the number of points in a simulation. Equation (18) weighs x_{error} and y_{error} equally and scales θ_{error} by a constant c . This allows the system to control whether it “prefers” error in the yaw direction compared to translational errors.

The sum is then multiplied by a time-varying weighting constant. This allows the WCE to weigh certain time intervals more heavily. For example, if the desire was to have the lowest steady state error, the final terms in the simulation trial would be weighed more heavily, implying that $\dot{w} > 0$. If the critical dimension was the rise time, the derivative of w would be negative, weighing the transient response more heavily.

3.3 Experimental Controller

The basic controller takes the over-actuated system and applies the constraint that the angles of the azimuthing thrusters are required to be equal. This leads to the following solutions for the actuator outputs:

$$F_1 = \frac{\sqrt{\underline{T}(1)^2 + \underline{T}(2)^2} + \frac{\underline{T}(3)}{l_2 \sin \alpha_1}}{(1 + l_1/l_2)} \quad (19)$$

$$F_2 = \sqrt{\underline{T}(1)^2 + \underline{T}(2)^2} - F_1 \quad (20)$$

$$\alpha_1 = \alpha_2 = \tan^{-1} \left(\frac{\underline{T}(2)}{\underline{T}(1)} \right) \quad (21)$$

where $\underline{T}(i)$ is the i th entry in the scaled error vector \underline{T} . The derivation of this result is shown in Appendix B.

The design of the controller leads the thrusters to always seek to the error vector defined by x and y errors. The torque to decay yaw errors is generated by the varying the forces applied by the thrusters. In order to tune this controller, the PID constants are varied, scaling the \underline{T} vector and shaping the system response.

By examination, F_1 and F_2 explodes when α_1 is small compared to $\underline{T}(3)$; this is the case where there is a heading error and the thrusters are in line with the kayak. In this position, they cannot generate corrective torques without applying a large thrust. Due to the positive only thrust constraint, the system pushes itself away from the original position into a more controllable configuration where it is able to correct itself.

4. Simulation Process and Results

The controllers were subjected to a series of step response tests. These include tests to see how both respond to errors in one, two and three degrees of freedom. Furthermore, by specifying desired locations that cause oscillations near the rotation limits of the thrusters, the nonlinear effects can be observed.

The PID constants are also varied in order to achieve the optimal response in specific orientations. This is achieved by iterating over the simulations with different values of proportional and derivative constants and measuring both the WCE and the settling time (see Appendix C). It is important to note that these constants rely heavily on the system parameters used by the model. They should be chosen to match the physical system as well as possible; the list of the parameters used in the model is shown in Table 1.

Table 1: List of parameters used throughout the simulated trials.

Parameter	Value	Units
m	45	kg
I	10	$kg\ m^2$
b_{surge}	.1	$N\ s/m$
b_{sway}	.5	$N\ s/m$
b_{yaw}	2	$N\ m\ s/rad$
l_1	.5	m
l_2	.5	m

Parameter	Value	Units
l_c	.2	m
dt	.01	s
ω_i	.5	rad/s
F_{max}	100	N
τ	.9	-
P	.5	-

4.1 Digression on Data Presentation

The kayaks behavior in three degrees of freedom is hard to convey easily on paper. Additionally, the body-referenced nature of the system tends for actuator outputs to be hard to understand intuitively and it's easy to get lost as the kayak maneuvers throughout the plane. To help mitigate that, the data is presented in three ways; an overall system error versus time plot, an actuator output plot, and an x-y plane with position and heading.

The thruster plots (shown below in Figure 4.2a) display the magnitude and direction of the forces produced *relative to the boat's heading*. The trajectory plot shows the general scheme of maneuver of the craft. The kayak images are not to scale and are *not* spaced as a function of time (although the times are noted). It is important to note the magnitude of the step response plots as they change between different configurations. A digression on the disturbance force application and generation can be found in Appendix D.

4.2 One and Two Degree of Freedom Step Responses

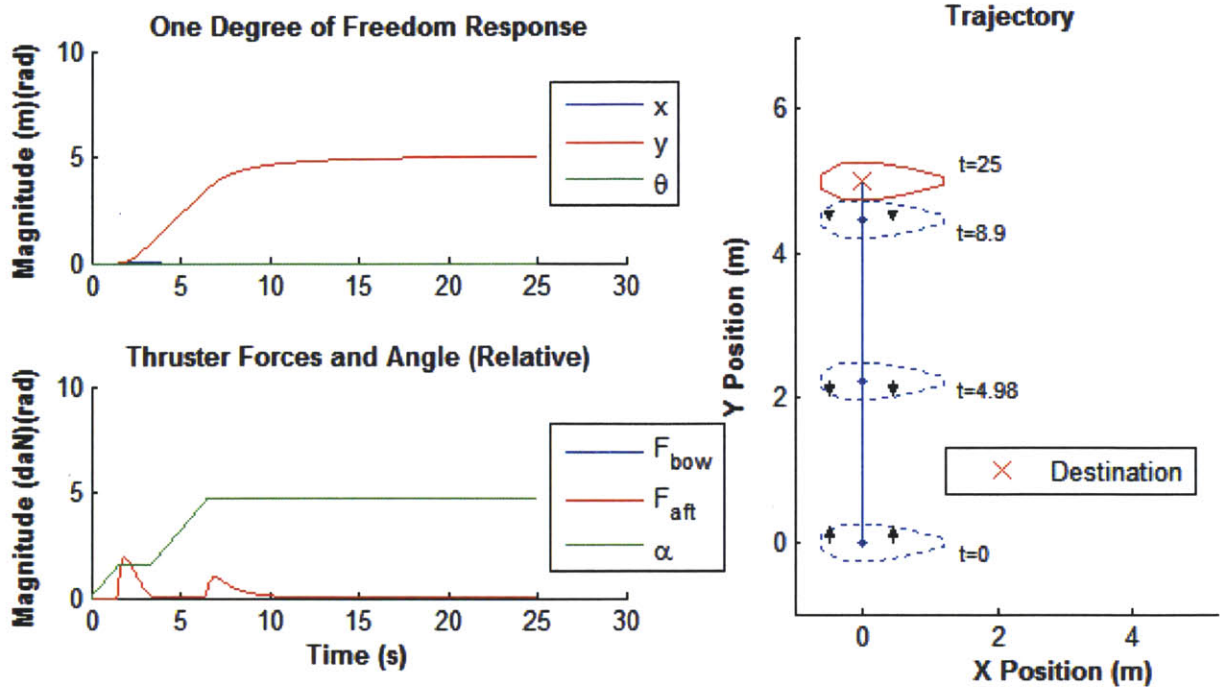


Figure 4.2a: One meter step response in the sway direction, settling to its final destination in under 20 seconds with under a millimeter precision. It exhibits an overdamped response. The azimuthing thrusters rotate into the opposite position prior to reaching the destination, preventing overshoot.

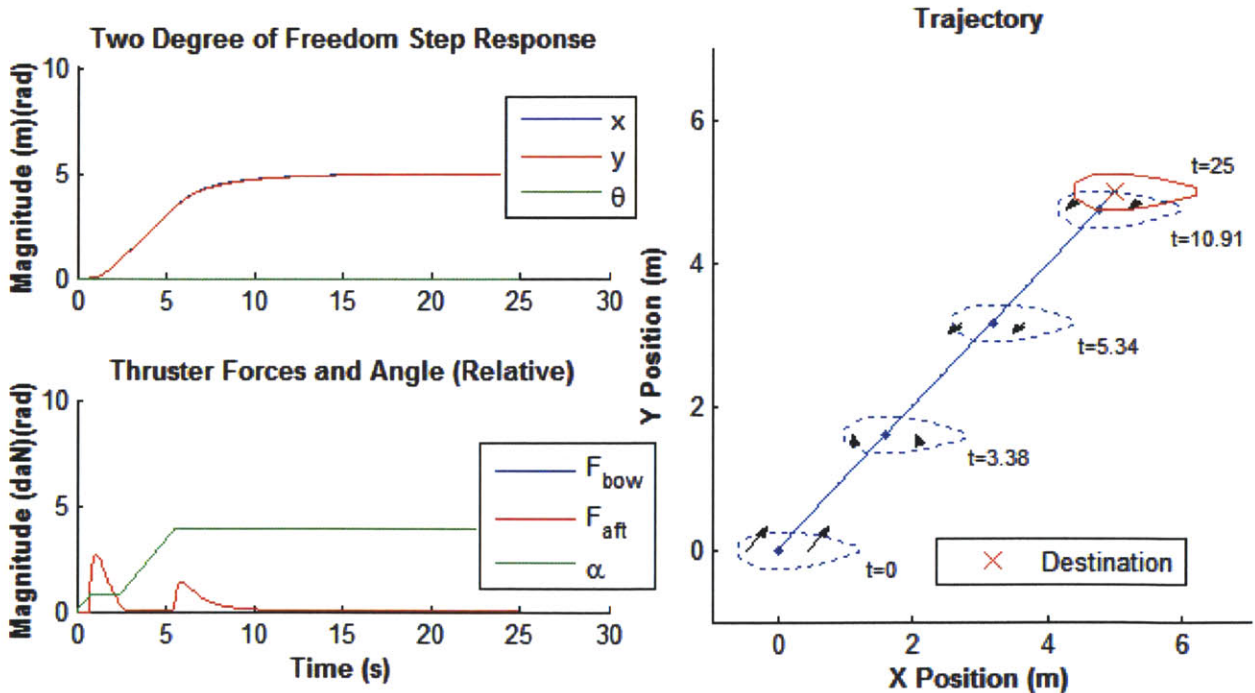


Figure 4.2b: Step response in both the sway and surge directions. The craft maintains its heading by producing the same force at both thrusters.

4.3 Oscillatory and Overdamped Responses in Three Degrees of Freedom

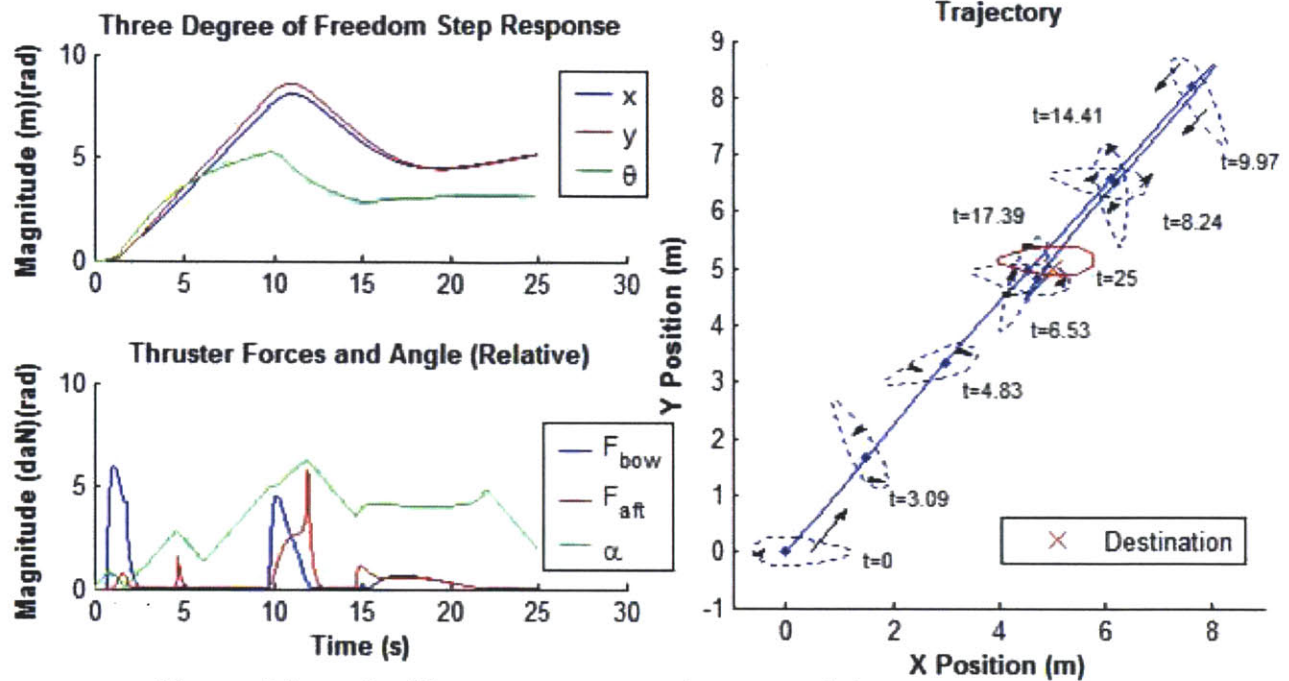


Figure 4.3a: Oscillatory response and commanded outputs to a three degree of freedom step input. The thruster magnitudes are not equal in order to produce the torque necessary to reduce the heading error.

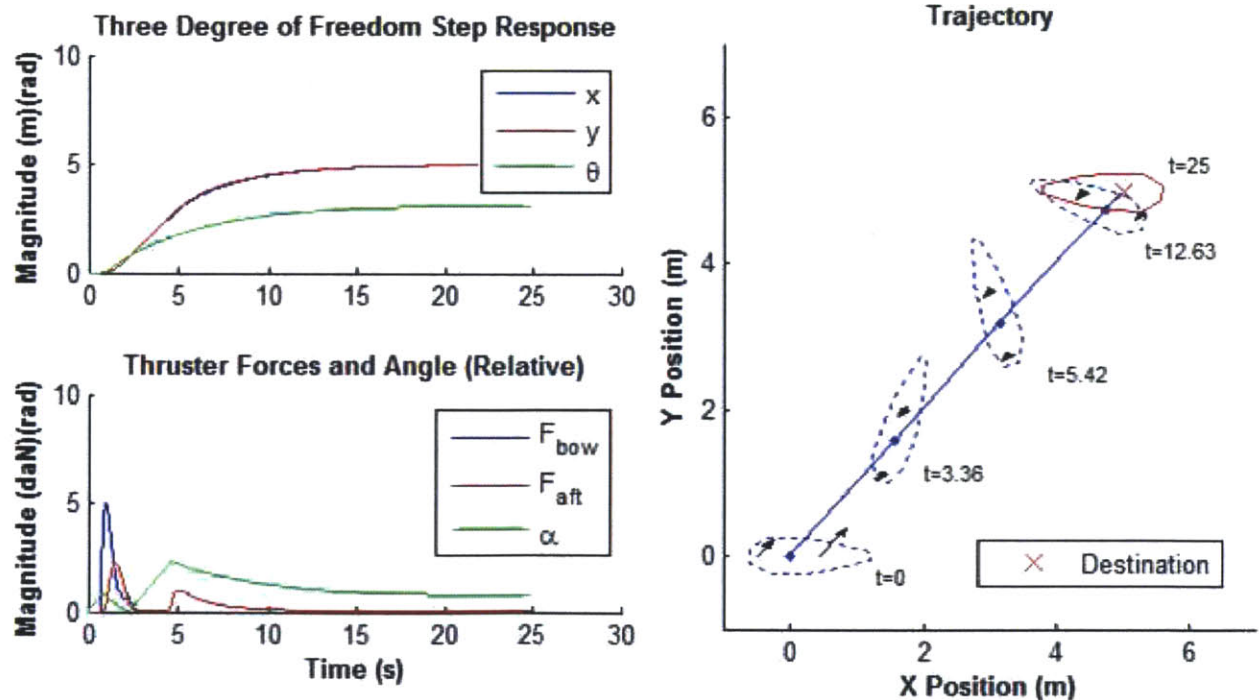


Figure 4.3b: The damped response follows a simpler trajectory towards the destination by using less thrust from the position error. Contrasting the overdamped actuator plot to the oscillatory one, the thruster angles and forces are more "behaved" here because it is preventing overshoot by initially driving the system less.

4.4 Response to Constant Disturbance Force

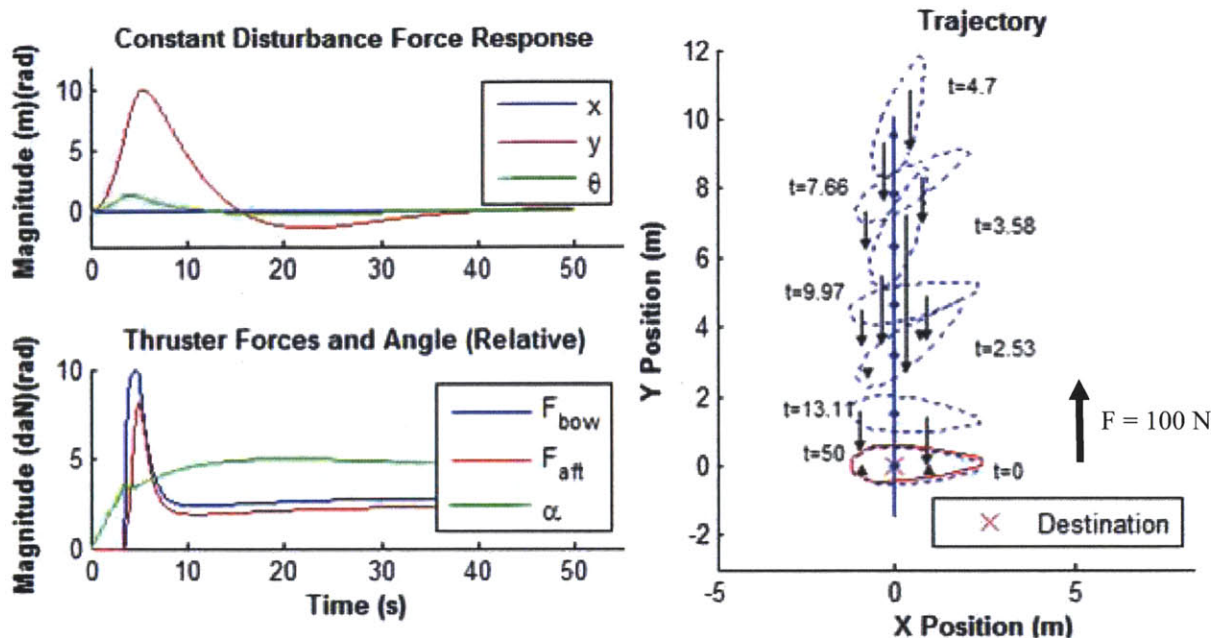


Figure 4.4a: A 100 N constant force drives the kayak in the y direction. The kayak “sees” the error once it is maneuvered out of position. Even after it settles back into position, the thrusters continue producing thrust to counter the disturbance force. Note that the bow thruster produces more thrust than the aft; this counters the torque that the force produces.

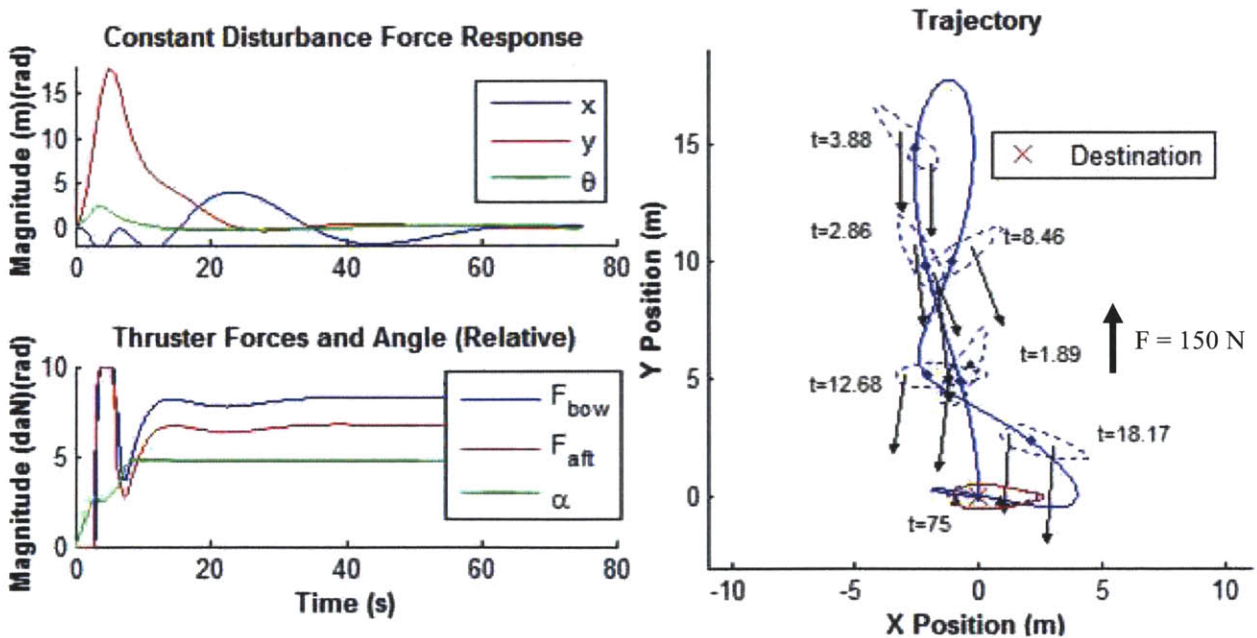


Figure 4.4b: Here, a larger (150 N) force in the same direction drives the kayak away from its destination. It recovers in a similar manner to before but it does undergo a more drastic trajectory and the thrusters reach their maximum capable output.

4.5 Response to Sinusoidal Disturbance Force

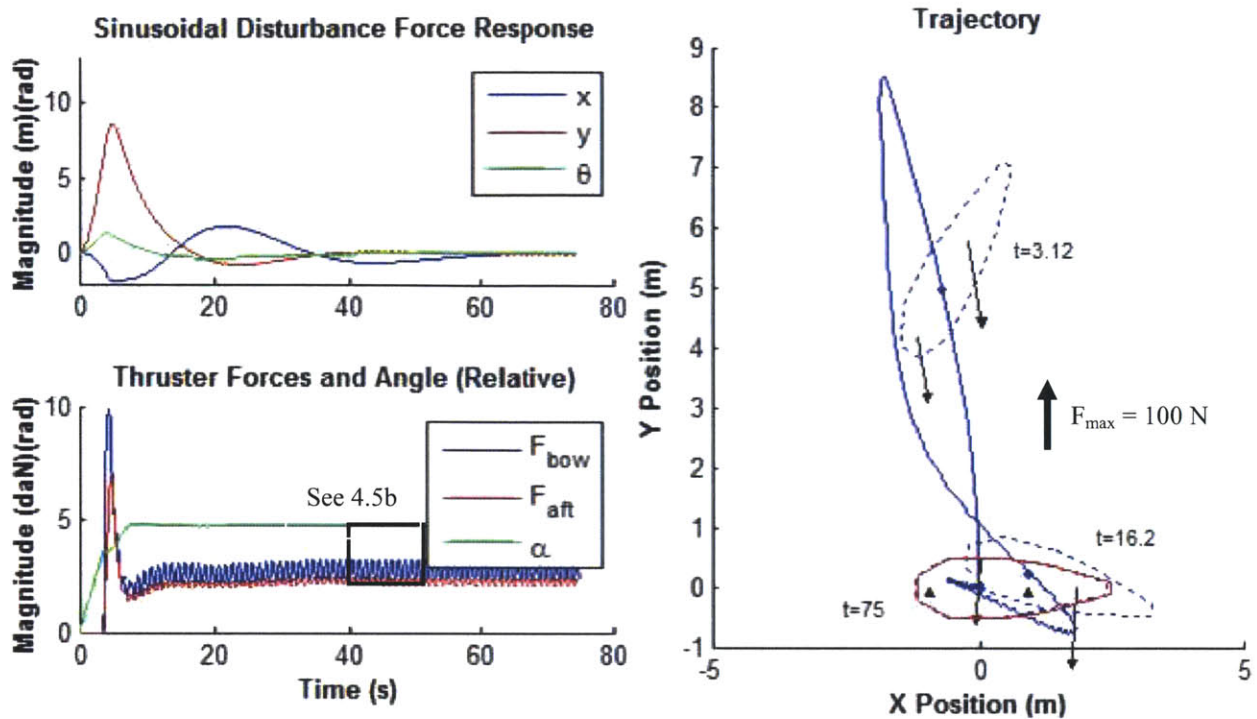


Figure 4.5a: Driving the system with a waveform models a wave disturbance force. A 100 N peak-to-peak, 1 Hz sinusoid drives the system in the y direction, eliciting an error in all three degrees of freedom. Furthermore, Figure 4.5b below shows the sinusoid propagating into both the position and thrusters.

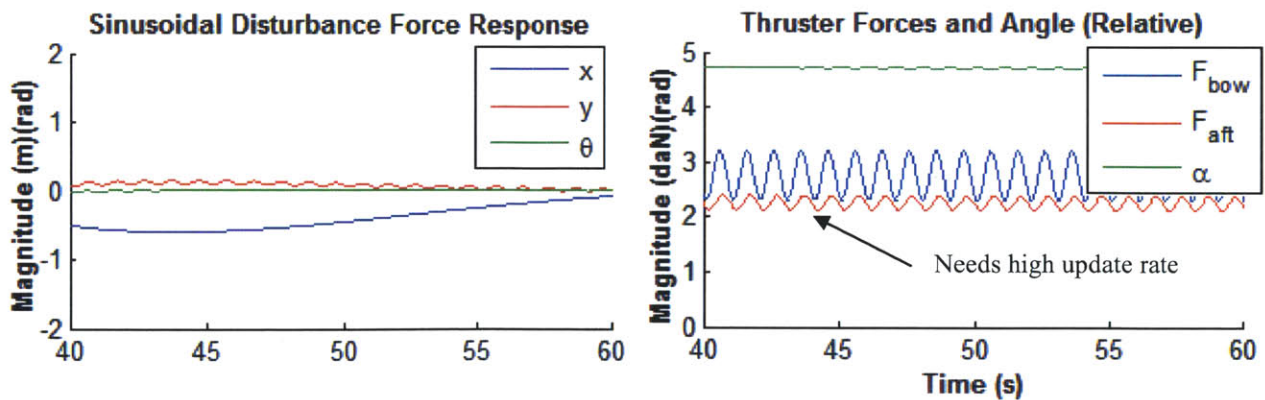


Figure 4.5b: 20-second snapshot of the steady-state response from a sinusoidal disturbance. The bow thruster consistently produces more force with larger amplitude because it is accommodating for both the translational and rotational forces that the disturbance induces. Note the controller resolution that is required to maintain position against this force.

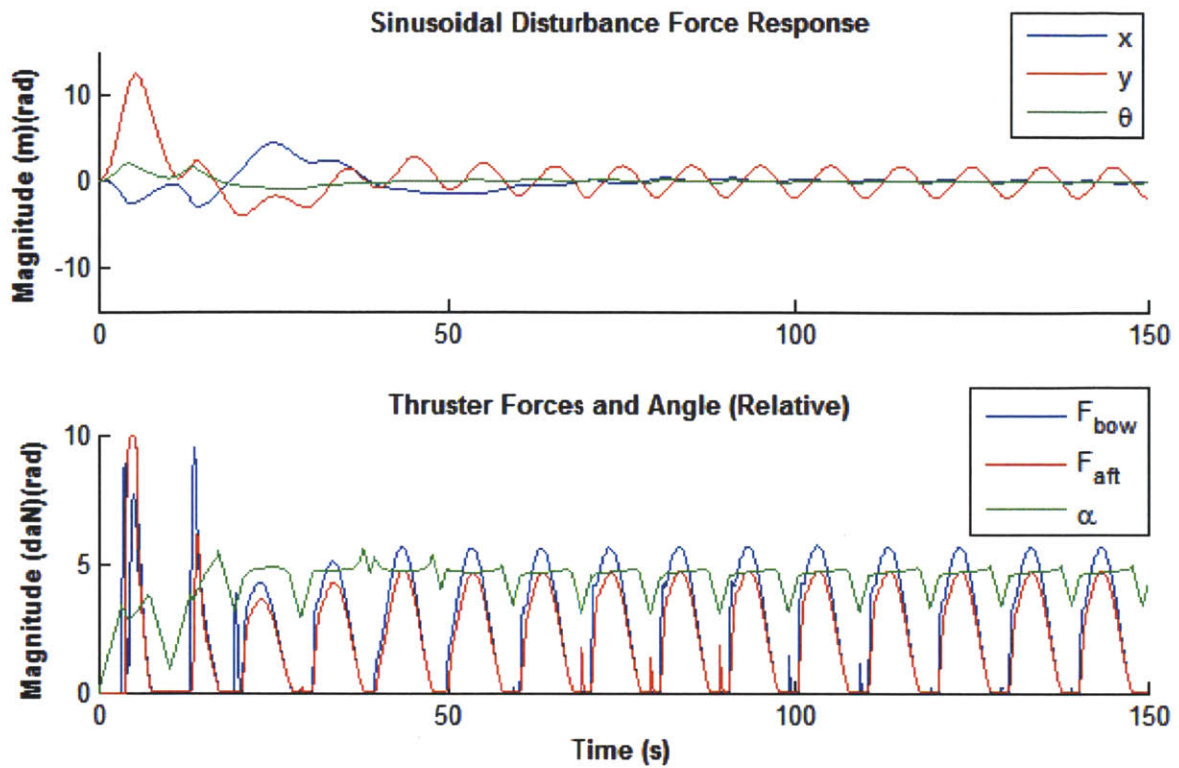


Figure 4.5c: Similar case where a lower frequency (.1 Hz) sine-wave drives the kayak. This produces an interesting transient response where the kayak oscillates around the goal location similar to the two degree of freedom step response. However, the actuator behavior in the steady state is more manageable.

4.6 Operation near Azimuthing Thruster Physical Stop

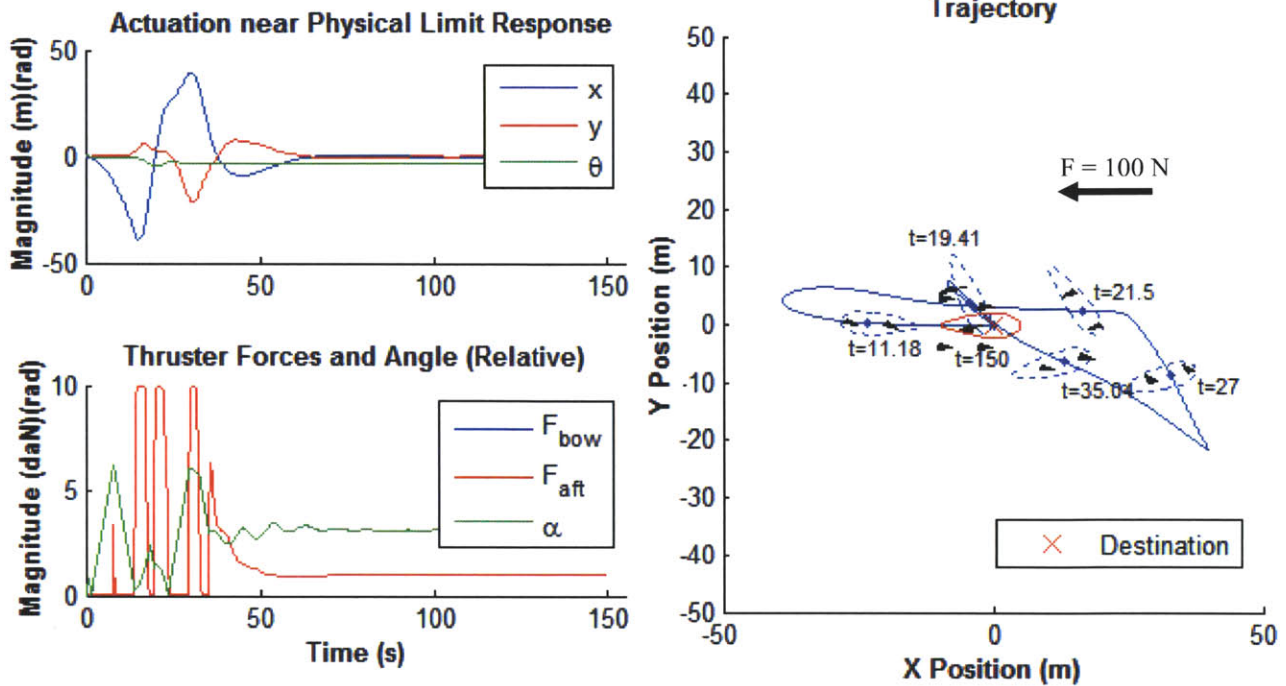


Figure 4.6a: A disturbance force with slight directional variance drives the kayak near the thruster's physical rotation limits. The θ constraint must be relaxed in order for the system to settle. The transient behavior arises from the poor control it has with the initial heading; it must be pushed into a controllable position.

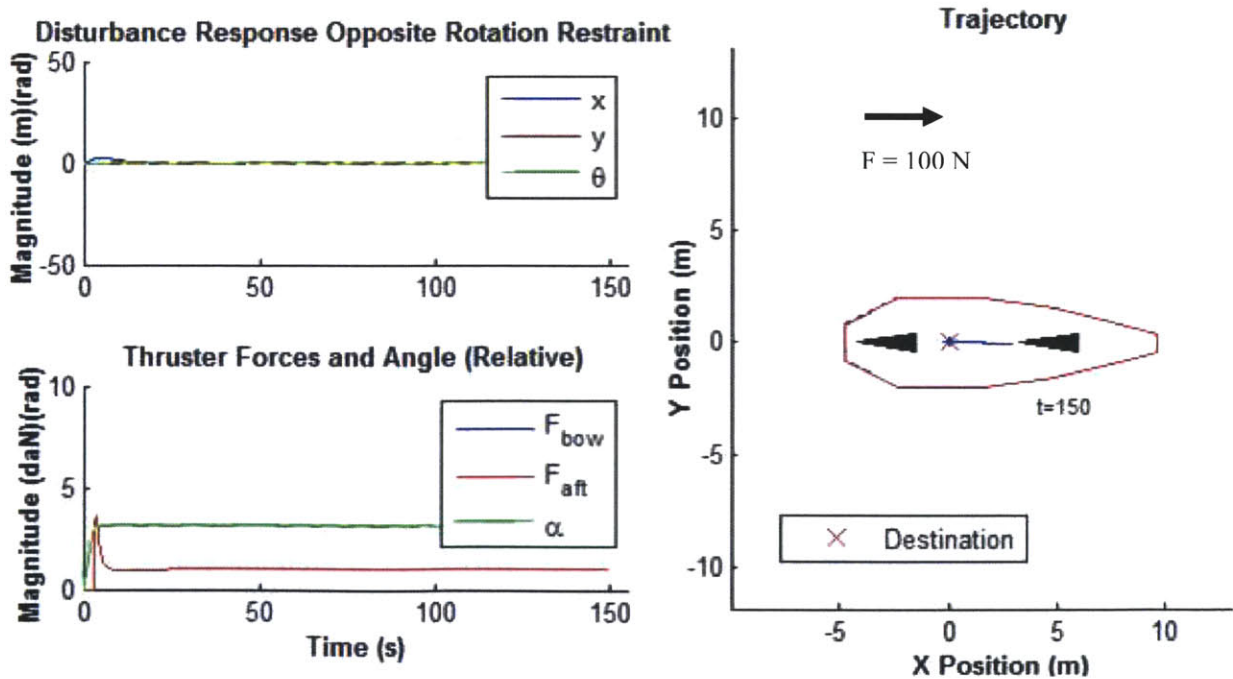


Figure 4.6b: The same force, now from the opposite direction, with negligible effect.

5. Analysis and Discussion

The simple nature of the controller provides a relatively easy and stable controller for stationkeeping. Some features are deceptively effective at controlling the behavior of the kayak despite their straightforward definitions. The few calculations and data that the controller must parse decreases the workload on the controller. However, as shown in some of the above figures, failure conditions do exist where the three degrees of freedom of the system cannot all be controlled simultaneously.

5.1 Predictive Behavior of the Azimuthing Thrusters

The calculation of the thruster angles from the scaled error vector \underline{T} :

$$\alpha_1 = \alpha_2 = \tan^{-1} \left(\frac{\underline{T}(2)}{\underline{T}(1)} \right) \quad (21)$$

accounts for the position of the kayak relative to its destination as well as its velocity towards it. This is handled by the proportional and derivative constants which shapes the kayaks behavior as it approaches its destination.

Figure 5.1 shows the kayak's azimuthing thrusters propelling it towards its destination calculated with only a proportional term.

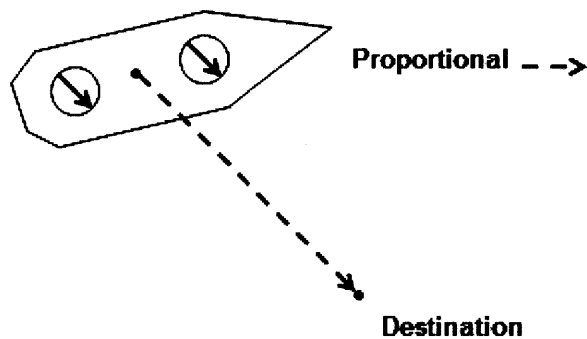


Figure 5.1: Simple P-controller which drives the kayak towards the destination according to the position error. This tends to oscillate around the destination due to low viscous forces that decay velocity slowly. Furthermore, the thrusters rotation around to the optimal direction increases settling time.

This has the (obviously) beneficial effect of driving it towards its destination. However, the kayak is only slowed by small viscous terms, tending it to overshoot its target. The thrusters are then forced to rotate into the opposite position to drive it back towards its destination. This continues, producing an oscillatory effect that is further compounded by the time the thrusters require to rotate after realizing the kayak overshoot its destination.

It seems obvious that the kayak should account for approaching its destination, but the best way to implement it is hard to know. Fortunately, the derivative constant in the error term adjusts for how rapidly the kayak is approaching its target as seen in Figure 5.2 below.

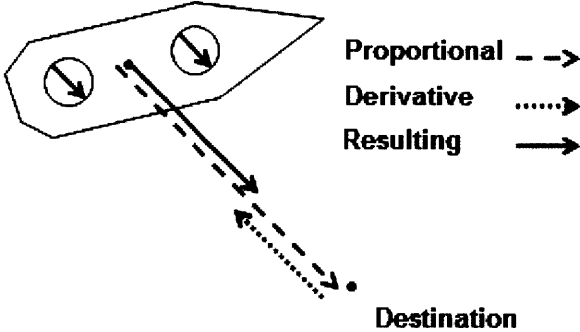


Figure 5.2: The PD-controller accounts for the velocity that the kayak approaches the destination with. This decreases the force generated by the thrusters, slowing its approach but saving time by reducing overshoot and oscillations.

This tends to decrease T , slowing its approach to the goal location by decreasing the amount of thrust produced. A more extreme case is show in Figure 5.3:

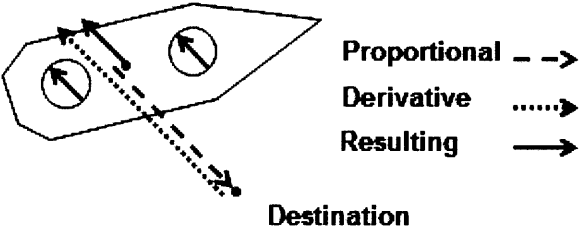


Figure 5.3: Although the kayak has not yet reached its destination, it has enough velocity that the controller begins to reverse thrust. The thrusters rotate to the opposite angle prior to overshooting, minimizing the amount of time it spends homing in on the destination.

Here, the proportional term is smaller than the derivative term and the resulting error vector is point away from the destination despite not having yet reached it. In order to produce the resulting output, the thrusters rotate to the new angle *prior* to overshooting it (due to the positive thrust constraint). From there, they slow the craft down until it eventually reaches its goal position.

5.2 Transient Error Reduction

One of the drawbacks of the experimental controller is that it always attempts to move the craft in the exact direction of the vector sum of x and y errors, α_{des} . The thrusters rotate to the necessary angle, at times passing through angles where, if they produced thrust, they would move the craft in a way that decreases one or more error term. However, since the thrusters had not reached the final angle, they do nothing.

An example of the principle is shown in Figures 5.4 and 5.5.

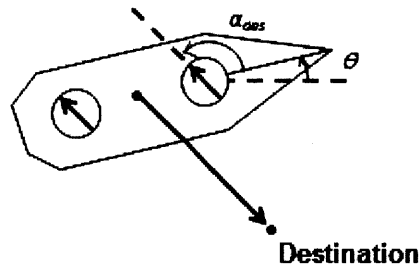


Figure 5.4: Desired thruster configuration specified by the benchmark controller for the destination vector shown.

Figure 5.4 shows the optimal angle α_{des} for the thrusters to be in order to reach a given destination. If, at some moment prior to that, the motors were in a position show in Figure 5.5 (shown below), it is apparent that driving the thrusters at that moment would alleviate the overall error within the system. In this case, it would decrease y -position error.

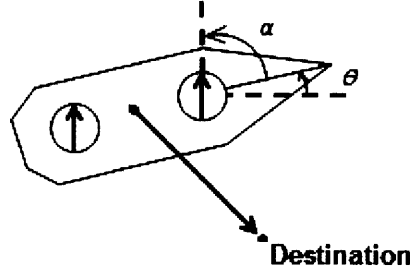


Figure 5.5: Moment in time prior to reaching the azimuthing angle goal. Producing thrust at this moment would decrease x_{error} while not increasing y error.

This could also be applied to the decrease heading error simply by choosing the thruster forces such that a desirable torque is produced.

If the craft did exhibit this behavior, it will result in the desired angle α_{des} to move as the kayak moves. This is not necessarily an undesirable outcome; it would occur in the actual implementation given disturbance forces in the system that would change α_{des} over time. Furthermore, it would alleviate the time-dependent nature of the thrusters as they would be allowed to scale up as they approach the desired angle.

5.3 Failure Conditions for the Controller

In certain situations, the physical limitations on the kayak limit the controller's performance. When the thrusters are constrained to operate at the same angle, the rotation stop on the thrusters creates an uncontrollable configuration, as shown in Section 4.6 above.

An easily overlooked flaw in the system is in the definition of the desired angle α_{des} .

$$\alpha_1 = \alpha_2 = \tan^{-1} \left(\frac{\underline{T}(2)}{\underline{T}(1)} \right) \quad (21)$$

Besides the fact that it is not well defined for when the error terms equal zero, it is a function solely of the planar scaled error terms. This does not describe the scenario where there is only heading error. If the system is not perturbed into creating non-zero $\underline{T}(1)$ or $\underline{T}(2)$ terms, the craft will never create a corrective torque (this problem is simple enough to fix but it is important to note its innate fault).

The limits on rotational speed inhibit the system in different ways. Most obviously, the time required to rotate into the proper angle adds a proportional amount of time to the settling time of the system. While not very significant for large disturbances, the precision control of the kayak is limited by its slow response.

The integral functionality of the controller also suffers. In the case where the thrusters instantaneously moved to the optimal angle, if the integral constant is set too high relative to the proportional and derivative constants, the system has a tendency to oscillate around its desired location simply because the integral term has not “reached” the optimal force to produce. However, when the system is forced to accommodate that rotation time, the controller integrates the error during that period into the integral term. This “extra” force tends to drive the system to oscillate even more; if the viscous terms (both physical and virtual) are not large enough, the system becomes unstable.

5.4 Thruster Response

The behaviors of the thrusters create instabilities within the system. Although this model assumes a very simplified thruster dynamic, this assumption includes physical effects that the thrusters would indeed exhibit. From the definition in the system dynamics above, the thrusters are assumed to behave as:

$$F_{i,t} = \tau F_{i,t-1} + (1 - \tau)\tilde{F}_{i,t} \quad (8)$$

$$\tau \in [0,1] \quad (9)$$

This time lag restricts the thrusters from outputting the optimal force output *if* the previous command were different. This comes into effect in the transient response of the kayak.

Lagged forces change the behavior of the system in two different ways. The most obvious is that the system is not outputting the proper size force. This could be in the form of under-producing when a large force is required and over-producing when the controller specifies a smaller one. The second case is where the forces are in the wrong direction. This is evident (though not significant) in the one degree of freedom step response in Figure 4.2a. In this case, there is initially only error in the y direction. As the system corrects the y error, it rotates to

produce force in the positive and negative y directions. As it begins to rotate to a new angle, the time lag produces a force in the x direction, producing error when there was originally none.

6. Conclusion

Stationkeeping is a necessary functionality of USVs. A stationkeeping controller must be able to accurately achieve a specific location and be robust to disturbance forces that seek to perturb it away. The problem posed by controlling three degrees of freedom with four outputs is an overactuated control problem that seems simple enough. However, nonlinearities inherent to the system's design and implementation restrict its capabilities.

An experimental controller was derived that sufficiently accommodated the limitations on the kayak system. The assumption that the thruster angles are always equal creates a holonomic system out of a redundant one. This simple implementation allows for the nonlinearities in the system to be studied more clearly and succinctly. The basic nature of the controller also allows for the physical system to be implemented relatively easily.

In response to three degree of freedom step inputs, the system was shown to be very stable in most configurations, achieving 5 meter translations and 180° heading changes with settling times under 20 seconds with under a centimeter fidelity. The system is more than capable of producing larger motions but the maximum thruster outputs are reached, increasing the amount of time it takes for larger motions.

However, this controller does not eliminate all problems within the system. In certain key configurations, the controllability of the kayak is lessened; this results in the need for either the kayak to be *pushed* into a controllable region or for controller constraints, such as the heading control, to be relaxed. In general, the kayak is capable of resisting large forces of approximately 75% of its maximum thrust output; the time lagged thrust behavior and rotational limitations account for the difference in forces.

This study provides a benchmark for future research into similar systems. The nonlinearities dealt with in this model are problems that countless nautical vehicles encounter; in general, the methodology discussed here follows a basic approach for characterizing *what* the system would do and *why* it fails. Further studies should be done in both increasing and decreasing the system constraints to understand not only how they behave, but how they behave in relation to each other.

7. Acknowledgements

Eternal thanks to Professor Franz Hover for his steadfast technical guidance throughout course of the semester, despite a constant lacking of early results on my part, attributed to both initial model failure and my own lethargy. Thanks also to graduate students Brooks Reed and Rob Hummel for providing continual support, answering questions, and nudging me in the correct direction in developing an appropriate model. Additional thanks to Professor Neville Hogan for initially pointing me in the right direction and keeping me on track. Final thanks to my friends and family who provided overall moral and physical support in not only the completion of this study, but throughout my entire MIT experience.

Appendix A: Formation of State Space Matrices

From the linear and angular momentum equations discussed above:

$$m\dot{u} - v\dot{\theta} = b_{surge}u + F_1 \cos \alpha_1 + F_2 \cos \alpha_2 + \delta_{surge} \quad (\text{A.1})$$

$$m\dot{v} + u\dot{\theta} = b_{sway}v + F_1 \sin \alpha_1 + F_2 \sin \alpha_2 + \delta_{sway} \quad (\text{A.2})$$

$$I_{\theta\theta}\ddot{\theta} = b_{yaw}\dot{\theta} + F_1 l_1 \sin \alpha_1 - F_2 l_2 \sin \alpha_2 + \delta_{yaw} \quad (\text{A.3})$$

and the definition of the overall state vector, \underline{x} , actuator outputs, \underline{u} :

$$\underline{x} = [u \quad v \quad \dot{\theta} \quad \alpha_1 \quad \alpha_2 \quad x \quad y \quad \theta]^T \quad (\text{A.4})$$

$$\underline{u} = \begin{bmatrix} F_1 \\ F_2 \\ \alpha_{des,1} \\ \alpha_{des,2} \end{bmatrix} \quad (\text{A.5})$$

The \underline{A} and \underline{F} can be arrived by solving for $\dot{\underline{x}}$ with respect to \underline{x} and \underline{u} :

$$\underline{A} = \begin{bmatrix} m^{-1}b_{surge} & 0 & m^{-1}v \\ 0 & m^{-1}b_{sway} & -m^{-1}u \\ 0 & 0 & I_{\theta\theta}^{-1}b_{sway} \\ 0 & 0 & 0 \\ 0 & 0 & 0 \\ \cos \theta & -\sin \theta & 0 \\ \sin \theta & \cos \theta & 0 \\ 0 & 0 & 1 \end{bmatrix} \quad (\text{A.6})$$

The \underline{A} matrix in general is sparsely populated (it is an 8x8 matrix but the last 5 columns are omitted). At the bottom left corner of the matrix is the transformation matrix that relates body-referenced velocities to absolute velocities, \underline{R} . It also contains nonlinear terms arising from the body-referenced frame, commonly known as centripetal force.

The \underline{F} matrix relates the surge, sway, and yaw motions to the actuator outputs as well as the many restrictions on the actuator outputs. It describes the actuator behavior as a result of the

system state and the controller commands. For the azimuthing thruster angles, it is constrained in the following ways:

$$|\dot{\alpha}_i| = \min \left(\left| \frac{\alpha_{error,i}}{dt} \right|, \omega_i \right) \quad (\text{A.7})$$

$$\alpha_i \in [0, 2\pi] \quad (\text{A.8})$$

The thrust is similarly constrained:

$$F_{i,t} = \tau F_{i,t-dt} + (1 - \tau) \tilde{F}_{i,t} \quad (\text{A.9})$$

$$F_i \in [0, F_{max}] \quad (\text{A.10})$$

In both sets of equations, the actuator output is a function of the previous actuator outputs. This adds to the order of the system, reducing the ability of the system to optimally achieve its control outputs. In other words, the system dynamics are related to the forces produced by the thrusters; the forces produced by the thrusters are related to forces produced in the previous instant in time.

Appendix B: Derivation of Controller Outputs

From the relationship between actuator outputs and scaled error:

$$\underline{T} = \underline{C} \underline{F} \quad (\text{B.1})$$

there are three output equations:

$$\underline{T}(1) = F_1 \cos \alpha_1 + F_2 \cos \alpha_2 \quad (\text{B.2})$$

$$\underline{T}(2) = F_1 \sin \alpha_1 + F_2 \sin \alpha_2 \quad (\text{B.3})$$

$$\underline{T}(3) = F_1 l_1 \sin \alpha_1 - F_2 l_2 \sin \alpha_2 \quad (\text{B.4})$$

Under the constraint that $\alpha_1 = \alpha_2$, equations (B.2) and (B.3) simplify to:

$$\underline{T}(1) = (F_1 + F_2) \cos \alpha \quad (\text{B.5})$$

$$\underline{T}(2) = (F_1 + F_2) \sin \alpha \quad (\text{B.6})$$

By dividing equation (B.2) by (B.3) and rearranging, the result for α is found:

$$\alpha_1 = \alpha_2 = \tan^{-1} \left(\frac{\underline{T}(2)}{\underline{T}(1)} \right) \quad (\text{B.7})$$

By inspection of equations (B.2) and (B.3):

$$\underline{T}(1)^2 + \underline{T}(2)^2 = (F_1 + F_2)^2 \cos^2 \alpha + (F_1 + F_2)^2 \sin^2 \alpha \quad (\text{B.8})$$

$$\underline{T}(1)^2 + \underline{T}(2)^2 = (F_1 + F_2)^2 \quad (\text{B.9})$$

$$\sqrt{\underline{T}(1)^2 + \underline{T}(2)^2} = F_1 + F_2 \quad (\text{B.10})$$

Solving for F_2 in equation (B.4):

$$\underline{T}(3) = F_1 l_1 \sin \alpha_1 - F_2 l_2 \sin \alpha_2 \quad (\text{B.4})$$

$$F_2 l_2 \sin \alpha_2 = F_1 l_1 \sin \alpha_1 - \underline{T}(3) \quad (\text{B.11})$$

$$F_2 = \frac{F_1 l_1 \sin \alpha_1 - \underline{T}(3)}{l_2 \sin \alpha_2} \quad (\text{B.12})$$

Substituting equation (B.12) into equation (B.10) yields:

$$\sqrt{\underline{T}(1)^2 + \underline{T}(2)^2} = F_1 + \frac{F_1 l_1 \sin \alpha_1 - \underline{T}(3)}{l_2 \sin \alpha_2} \quad (\text{B.13})$$

$$F_1 \left(1 + \frac{l_1}{l_2}\right) = \sqrt{\underline{T}(1)^2 + \underline{T}(2)^2} + \frac{\underline{T}(3)}{l_2 \sin \alpha_2} \quad (\text{B.14})$$

$$F_1 = \frac{\sqrt{\underline{T}(1)^2 + \underline{T}(2)^2} + \frac{\underline{T}(3)}{l_2 \sin \alpha_2}}{\left(1 + \frac{l_1}{l_2}\right)} \quad (\text{B.15})$$

$$F_2 = \sqrt{\underline{T}(1)^2 + \underline{T}(2)^2} - F_1 \quad (\text{B.16})$$

Appendix C: Example PID Constant Iterations

In order to properly shape the system response, it is necessary to observe the relationship between the system behavior and the controller constants. In classical 2nd order systems, it is easy to design given the easy derivable (or tabulated) characteristics of settling time, rise time, percent overshoot, etc. However, in the kayak system, nonlinearities cannot be accounted for in observing the system, so it is necessary to generate plots of useful characteristics.

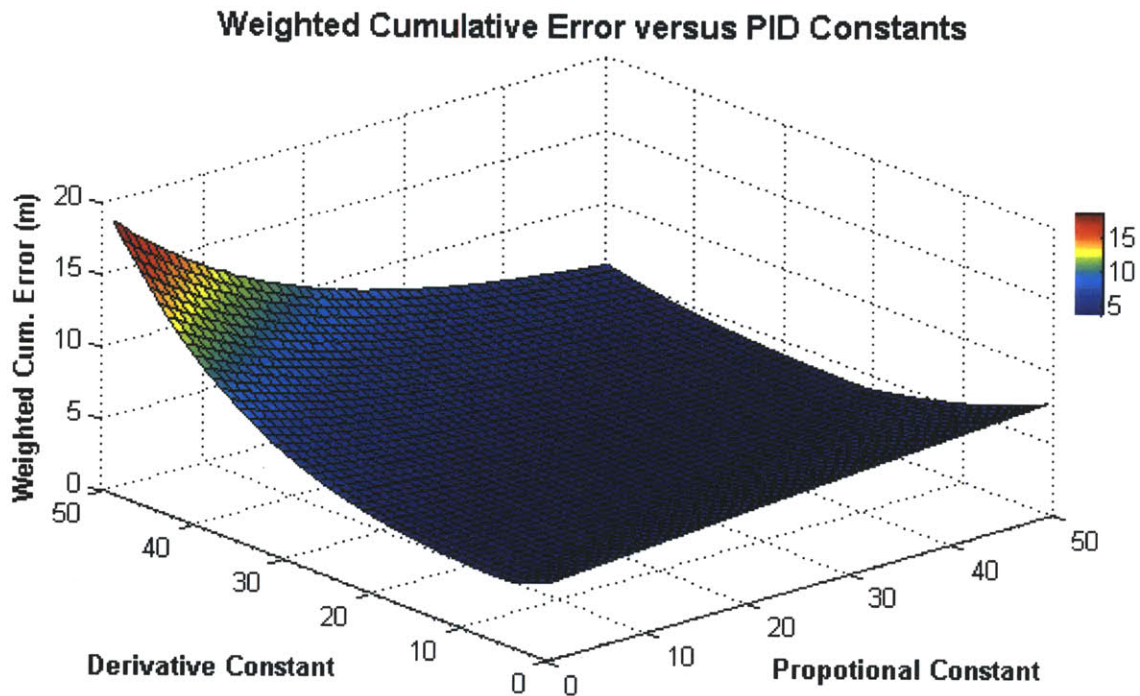


Figure C.1: Weighted cumulative error with $c=.5$ and $w(t)=1$. The constants are normalized.

It might seem trivially obvious to select the constants with the lowest WCE. However, the choice of the WCE constants weights all error equally over time (with half yaw error). This could result in the situation where the system quickly reaches its destination but oscillates around the result (a behavior we may not like). Figure C2 shows a settling time versus constants plot:

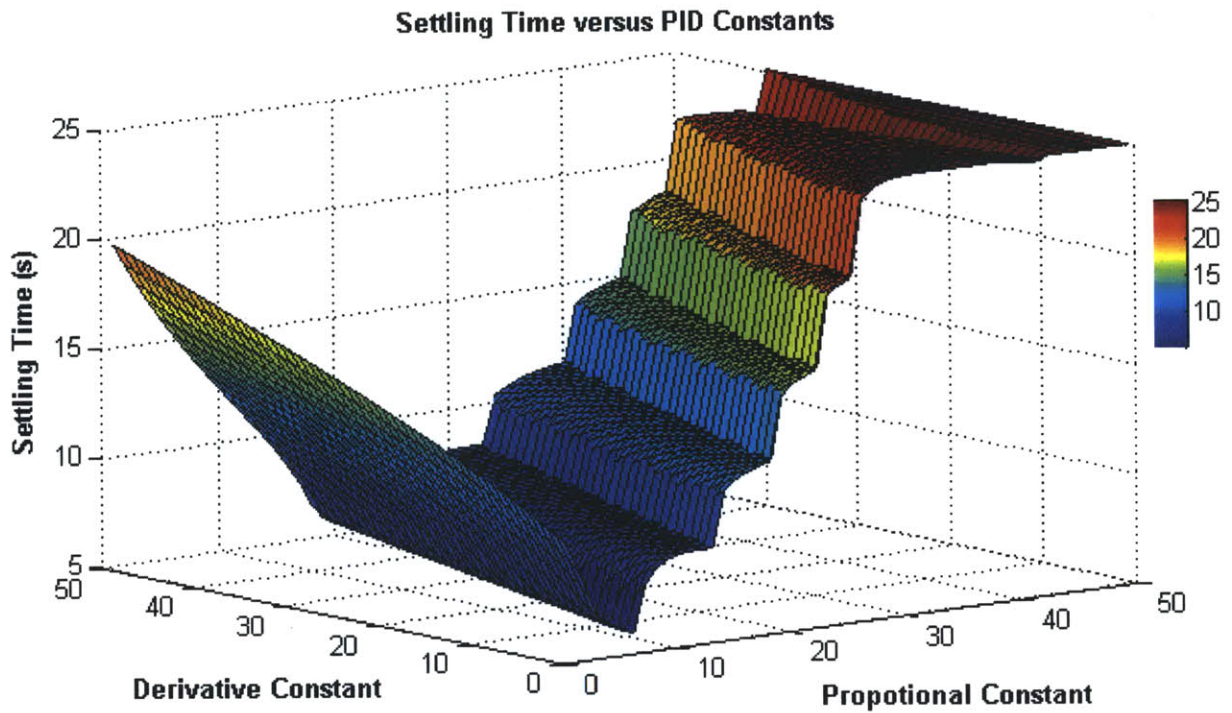


Figure C.2: Settling time defined as reaching 3% of all degrees of freedom. It is apparent that optimal values in Figure C1 are not so optimal if we willing to trade some WCE for a shorter settling time. Looking at the graph, the side to the right of the value corresponds to higher proportional terms and thus oscillatory response. The stepped nature is due to these oscillations; the peak amplitude is just enough to reach the 3% settling time criterion. The left hand side corresponds to overdamped responses.

Appendix D: Application and Formation of Disturbance Forces

The generation and application of environmental-based disturbance forces is necessary for understanding the behavior of the system in actual implementation. These forces are defined in a Cartesian frame and rotated appropriately into the surge, sway, and yaw dynamic equations. For a disturbance force $\underline{\delta}$ composed of an x and y forces:

$$\delta_{sway} = \delta_x \cos \theta + \delta_y \sin \theta \quad (\text{D.1})$$

$$\delta_{surge} = P(\delta_x \sin \theta + \delta_y \cos \theta) \quad (\text{D.2})$$

$$\delta_{yaw} = l_c \delta_x \cos \theta - l_c \delta_y \sin \theta \quad (\text{D.2})$$

where P is a correction factor arising from the larger profile presented in the sway direction relative to the surge direction. P is on the interval:

$$P \in [0,1] \quad (9)$$

It is important to see that a yaw disturbance force arises from the fact that the center of mass of the system is not at the center of the kayak (denoted by l_c).

Three different profiles of forces are used in this study; a constant, uni-directional force; a constant, varied-directional force; and a uni-directional sinusoidal force.

Constant Uni-Directional Force

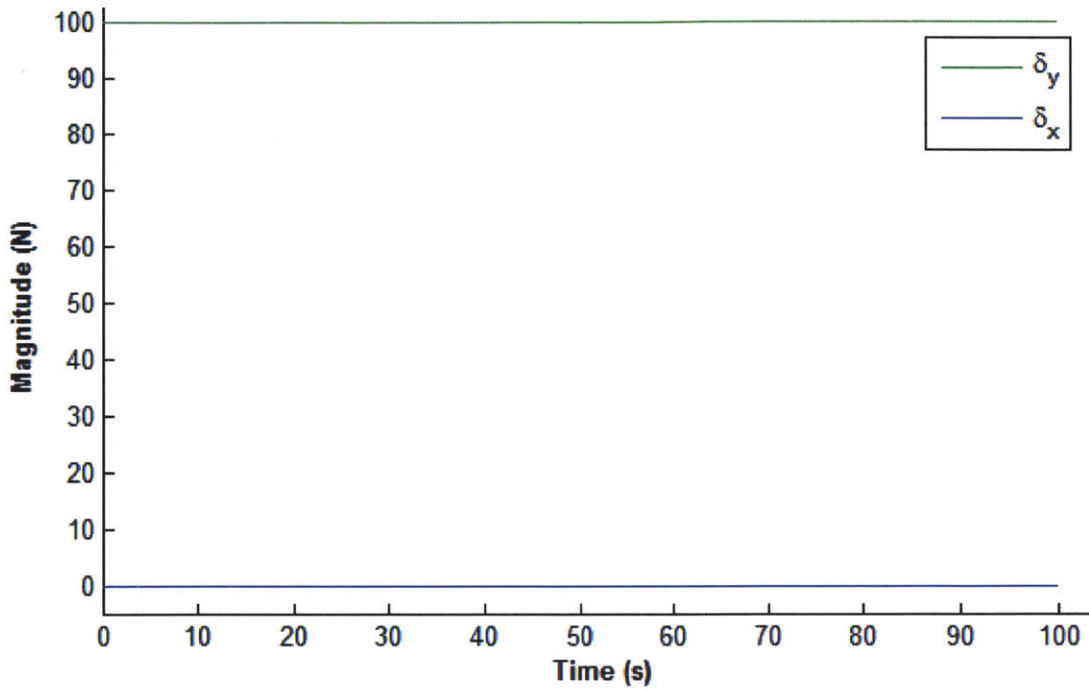


Figure D.1: Example of a constant, 100 N disturbance force being applied in only the y direction.

Directionally Varied Force

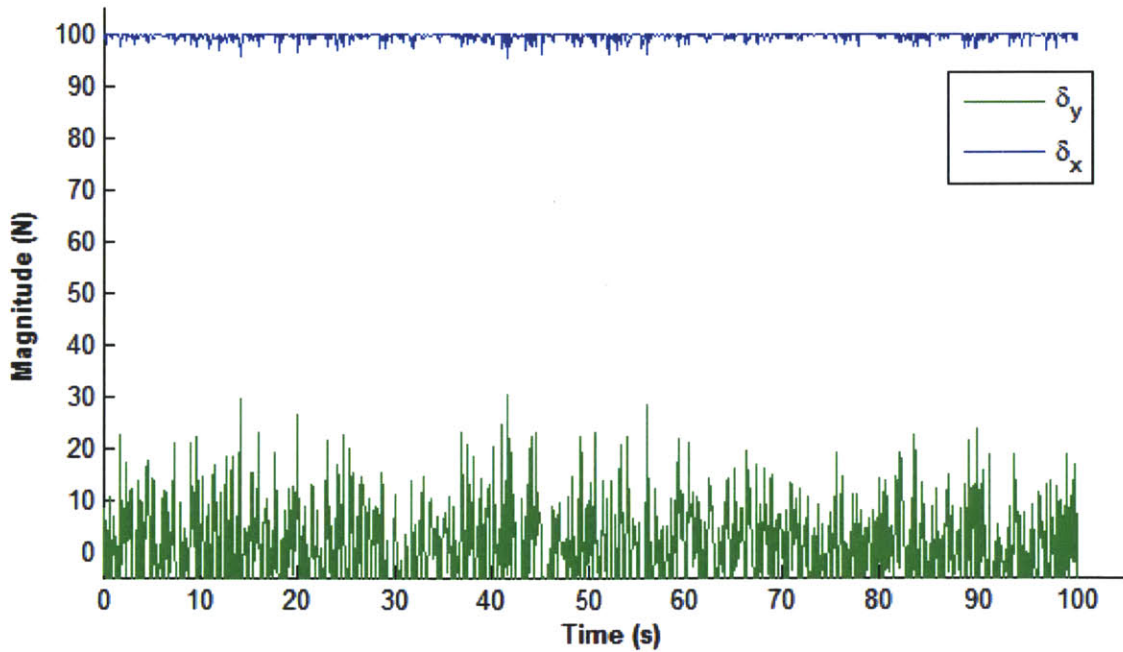


Figure D.2: Directionally varied force where applied in the positive x direction. Small forces in y tend to drive the kayak away from the y in order to test how the craft reacts to large errors in x and small, unpredictable errors in y.

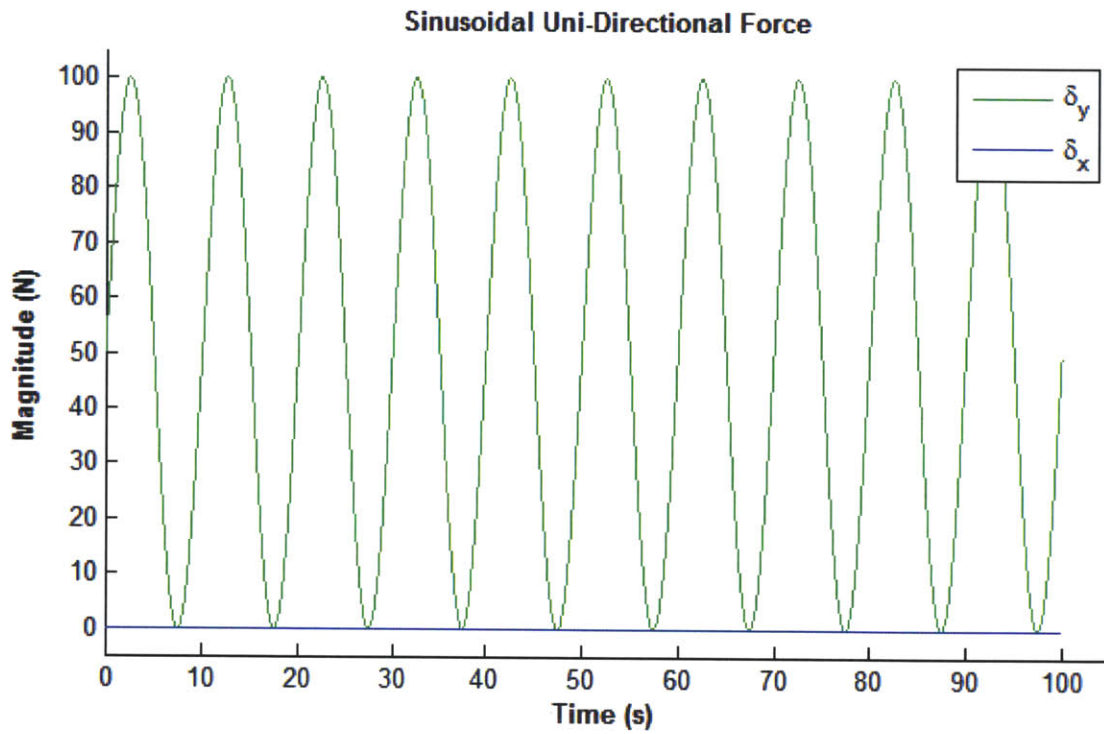


Figure D.3: Example of a sinusoidal force applied in only the y direction. This has a peak-to-peak value of 100 N with a mean value of 50 N. This example is driven at .1 Hz.